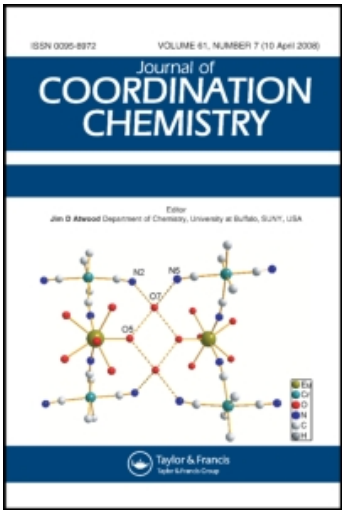

Journal of Coordination Chemistry
Publication details, including instructions for authors and subscription information:
http://www.informaworld.com/smpp/title~content=t713455674

Synthesis, characterization, and biological activity studies of copper(II)-metal(II) binuclear complexes of dipyridylglyoxal *bis*(2-hydroxybenzoyl hydrazone)

Ali El-Dissouky[a]; Othman Al-Fulaij[a]; Mohamed K. Awad[b]; Sayed Rizk[a]
[a] Faculty of Science, Chemistry Department, Kuwait University, Safat 13060, State of Kuwait [b] Faculty of Science, Chemistry Department, Theoretical Applied Chemistry Unit, Tanta University, Tanta, Egypt

First published on: 30 October 2009

To cite this Article El-Dissouky, Ali , Al-Fulaij, Othman , Awad, Mohamed K. and Rizk, Sayed(2010) 'Synthesis, characterization, and biological activity studies of copper(II)-metal(II) binuclear complexes of dipyridylglyoxal *bis*(2-hydroxybenzoyl hydrazone)', Journal of Coordination Chemistry, 63: 2, 330 — 345, First published on: 30 October 2009 (iFirst)
To link to this Article: DOI: 10.1080/00958970903366959
URL: http://dx.doi.org/10.1080/00958970903366959

Journal of Coordination Chemistry
Vol. 63, No. 2, 20 January 2010, 330–345

Taylor & Francis
Taylor & Francis Group

Synthesis, characterization, and biological activity studies of copper(II)–metal(II) binuclear complexes of dipyridylglyoxal *bis*(2-hydroxybenzoyl hydrazone)

ALI EL-DISSOUKY*†, OTHMAN AL-FULAIJ†, MOHAMED K. AWAD‡ and SAYED RIZK†

†Faculty of Science, Chemistry Department, Kuwait University, P.O. Box 5969, Safat 13060, State of Kuwait
‡Faculty of Science, Chemistry Department, Theoretical Applied Chemistry Unit, Tanta University, Tanta, Egypt

(*Received 30 July 2009; in final form 12 August 2009*)

A new series of copper(II) mononuclear and copper(II)–metal(II) binuclear complexes $[(H_2L)Cu]\cdot H_2O$, $[CuLM]\cdot nH_2O$, and $[Cu(H_2L)M(OAc)_2]\cdot nH_2O$, $n = 1$–2, M = Co(II), Ni(II), Cu(II), or Zn(II), and L is the anion of dipyridylglyoxal *bis*(2-hydroxybenzoyl hydrazone), H_4L, were synthesized and characterized. Elemental analyses, molar conductivities, and FT-IR spectra support the formulation of these complexes. IR data suggest that H_4L is dibasic tetradentate in $[(H_2L)Cu]\cdot H_2O$ and $[Cu(H_2L)M(OAc)_2]\cdot nH_2O$ but tetrabasic hexadentate in $[CuLM]\cdot nH_2O$ ($n = 1$–2). Thermal studies indicate that waters are of crystallization and the complexes are thermally stable to 347–402°C depending upon the nature of the complex. Magnetic moment values indicate magnetic exchange interaction between Cu(II) and M(II) centers in binuclear complexes. The electronic spectral data show that d–d transitions of CuN_2O_2 in the mononuclear complex are blue shifted in binuclear complexes in the sequences: Cu–Cu > Cu–Ni > Cu–Co > Cu–Zn, suggesting that the binuclear complexes $[CuLM]\cdot nH_2O$ are more planar than the mononuclear complex. The structures of complexes were optimized through molecular mechanics applying MM^+ force field coupled with molecular dynamics simulation. $[(H_2L)Cu]\cdot nH_2O$, $[CuLM]\cdot nH_2O$, and the free ligand were screened for antimicrobial activities on some Gram-positive and Gram-negative bacterial species. The free ligand is inactive against all studied bacteria. The screening data showed that $[CuLCu]\cdot H_2O > [(H_2L)Cu]\cdot H_2O > [CuLZn]\cdot H_2O > [CuLNi]\cdot 2H_2O \approx [CuLCo]\cdot H_2O$ in order of biological activity. The data are discussed in terms of their compositions and structures.

Keywords: 2,2′-Bipyridine; Homo- and hetero-binuclear complexes; Spectra; Magnetism; Biological activity

1. Introduction

The search for new synthetic routes to multimetallic complexes is pertinent in coordination chemistry and crystal engineering [1]. Interest in polynuclear complexes is stimulated by the relevance of these compounds in molecular magnetism, material

*Corresponding author. Email: alieldissouky70@yahoo.com

ISSN 0095-8972 print/ISSN 1029-0389 online © 2010 Taylor & Francis
DOI: 10.1080/00958970903366959

sciences, industrial catalysis, and bioinorganic chemistry, and they are ubiquitous in nature as active sites in a variety of metalloenzymes [1–7]. Polynuclear complexes provide understanding of the fundamental science of magnetic interactions, the factors affecting the sign and the magnitude of the intramolecular magnetic exchange interactions between identical or different paramagnetic centers and magneto-structural correlations in molecular systems. The synthesis of polynuclear complexes requires coordination complexes which present themselves as potential chelating ligands with more than one set of donor atoms [7]. ''Flexidentate'' ligands facilitate stepwise incorporation of further transition metal complex fragments giving multimetallic complexes. An efficient synthetic route in designing multimetallic complexes is the building block approach consisting of the use of complexes with bridging groups that will act as ligands toward a second metal ion. The choice of a non-linear bridging unit with coordination number greater than two increases dimensionally in the process [1, 8]. Several polynuclear complexes of the types A_2, A_3, AB, and ABA (A and B represent two different metal ions) were reported [2, 3, 7–10]. In this work, we synthesize and characterize the N/O multidentate chelating ligand dipyridylglyoxal *bis*(2-hydroxybenzoyl hydrazone), H_4L, and its mononuclear, homo- and heterobinuclear complexes.

2. Experimental

All reagents were purchased from Aldrich Chemical Company and used without purification. *N*,*N*′-Dimethylformamide (DMF) was distilled over molecular sieves and anhydrous $MgSO_4$ prior to use.

2.1. *Synthesis of dipyridylglyoxal bis(2-hydroxybenzoyl hydrazone), H_4L*

α-Pyridoin (4.28 g, 0.02 mol) was added to a methanolic solution (70 mL) of *o*-hydroxybenzoylhydrazine (6.08 g, 0.04 mol) was added in the same solvent (50 mL) in a round-bottom flask (250 mL). To this mixture, 4–6 drops of concentrated HCl were added and the mixture was stirred under reflux on a water bath for 18 h (during which the reaction was checked by TLC). The solvent was rotovaporated to half of its original volume and left to stand overnight at room temperature. The solid product was filtered off, washed several times with MeOH followed by Et_2O and recrystallized from $C_2H_4Cl_2$ to give a pale yellow crystalline product (yield 79.8%) with melting point (m.p.) of 199.8°C ± 1°C. The purity of the product was indicated by its sharp m.p., TLC test, and elemental analysis (table 1). ^{1}H NMR in d_6-DMSO: phenyl protons: δ 7.94 (2H), 7.34 (2H), 7.33 (2H), 6.93 (1 H), 6.86 (1 H); pyridine protons: δ 8.40 (2H), 8.27 (2H), 7.98 (1 H), 7.96 (1 H), 7.40 (2H); OH-protons: δ 12.70 (phenolic OH, hydrogen bonded), δ 10.98 (enolic OH, hydrogen bonded).

2.2. *Synthesis of the complexes*

2.2.1. $[(H_2L)Cu]\cdot H_2O$. A methanolic solution (20 mL) of $Cu(OAc)_2\cdot H_2O$ (0.20 g, 0.001 mol) was added to a suspension of H_4L (0.48 g, 0.001 mol) in methanol (30 mL).

Table 1. Elemental analysis, % yield, and color of H_4L and its complexes.

Compound	Yield (%)	Color	Analytical data (%) (found (% Calcd))				
			C	H	N	Cu	M
H_4L	79.8	Pale yellow	65.09 (65.00)	4.31 (4.17)	17.36 (17.50)		
$[(H_2L)Cu]\cdot H_2O$	89.6	Green	55.83 (55.76)	3.71 (3.57)	14.87 (15.01)	11.24 (11.36)	
$[CuLCu]\cdot H_2O$	93.5	Olive green	47.88 (47.48)	3.66 (3.35)	13.00 (12.78)	19.21 (19.34)	
$[CuLCo]\cdot H_2O$	76.9	Blue-green	47.96 (47.82)	3.24 (3.37)	13.00 (12.87)	9.81 (9.74)	9.21 (9.03)
$[CuLNi]\cdot 2H_2O$	80.4	Green	49.07 (49.19)	3.28 (3.15)	13.41 (13.24)	10.24 (10.02)	9.45 (9.25)
$[CuLZn]\cdot H_2O$	78.9	Green	50.42 (50.08)	3.00 (2.89)	13.29 (13.48)	10.11 (10.20)	10.61 (10.50)
$[Cu(H_2L)Cu(OAc)_2]\cdot H_2O$	91.5	Brown	48.23 (48.58)	3.42 (3.51)	11.00 (11.33)	17.35 (17.15)	
$[Cu(H_2L)Co(OAc)_2]\cdot H_2O$	77.3	Dark brown	49.01 (48.88)	3.42 (3.53)	11.33 (11.41)	8.60 (8.63)	8.23 (8.00)
$[Cu(H_2L)Ni(OAc)_2]\cdot 2H_2O$	81.0	Brown	47.94 (47.73)	3.80 (3.71)	11.00 (11.14)	8.50 (8.42)	8.00 (7.78)

The reaction medium was stirred under reflux on a water bath for 6 h, the solvent evaporated to half of its original volume, the green solid was filtered off, washed several times with MeOH and Et_2O, and dried *in vacuo* over P_4O_{10}.

2.2.2. [CuLCu]·H_2O. This complex was synthesized as described for $[(H_2L)Cu]\cdot H_2O$ but with using a mole ratio of 2:1 ($Cu(OAc)_2\cdot H_2O : H_4L$), yield 82.6%. Another method was also applied, solid $[(H_2L)Cu]\cdot H_2O$ (0.005 mol) was added to a methanolic solution (60 mL) of $Cu(OAc)_2\cdot H_2O$ (0.005 mol). The reaction mixture was stirred under reflux on a water bath for 20 min and the solution was filtered hot to remove all unreacted solid and refluxed for further 30 min. The solution was left overnight at room temperature and the olive green solid formed was filtered off, washed several times with MeOH and Et_2O, and dried *in vacuo* over P_4O_{10}.

2.2.3. [CuLM]·nH_2O, M = Co^{2+}, Ni^{2+}, or Zn^{2+} and n = 1–2. These complexes were synthesized by the same general method, namely, a methanolic solution (40 mL) of $M(OAc)_2\cdot nH_2O$, M = Co^{2+}, Ni^{+2}, or Zn^{+2} (0.005 mol) at 5–10°C was added dropwise with stirring to a suspension of $[CuLCu]\cdot H_2O$ (0.005 mol) in the same solvent (30 mL) at 0–5°C. After complete addition, the mixture was stirred for 15–30 min (at 5–10°C) during which the reaction was completed as shown from the complete color change and TLC tests. The reaction product in each case was filtered off, washed several times with cold MeOH and Et_2O, and dried *in vacuo* over P_4O_{10}. If the reaction was carried out at room temperature or under boiling conditions, a mixture of $[CuLM]\cdot nH_2O$ and $[MLM]\cdot nH_2O$ was obtained.

2.2.4. [Cu(H_2L)M($OAc)_2$]·nH_2O, M = Cu^{2+}, Co^{2+}, or Ni^{2+} and n = 1 or 2.
Method A: These were synthesized by the addition of solid $M(OAc)_2\cdot nH_2O$ (0.005 mol), M = Cu^{2+}, Co^{2+}, or Ni^{2+} to $[(H_2L)Cu]\cdot H_2O$ (0.005 mol) in MeCN (100 mL) followed by the addition of 3–5 drops of HOAc at 5–10°C. The reaction mixture was stirred for 2–3 h at 5–10°C and then left overnight at room temperature. The product in each case was isolated by filtration, washed several times with cold MeOH and Et_2O, and dried *in vacuo* over P_4O_{10}. Carrying out this reaction at room temperature or under boiling conditions lead to the formation of unresolvable mixture of products.

Method B: These acetato containing complexes were obtained by boiling a suspension of $[CuLM]\cdot nH_2O$, M = Co^{2+} or Ni^{2+}, and n = 1–2 in MeOH with NaOAc : HOAc (1 : 3, m/m) in a mole ratio of 1:2 (complex: OAc^-) for 3–5 h. The reaction routes are presented in figure 1.

2.3. *Physical measurements and elemental analyses*

C, H, and N analyses were obtained using a LECO CHNS-932 Elemental Analyzer. FT-IR spectra of the ligand and its complexes were recorded as KBr discs with a Perkin Elmer System 2000 FT-IR spectrophotometer. NMR spectra of the ligand in d_6-DMSO in the absence and presence of D_2O was performed with a Bruker DPX 400, NMR spectrometer. Electronic spectra of the ligand and their complexes either as nujol mulls

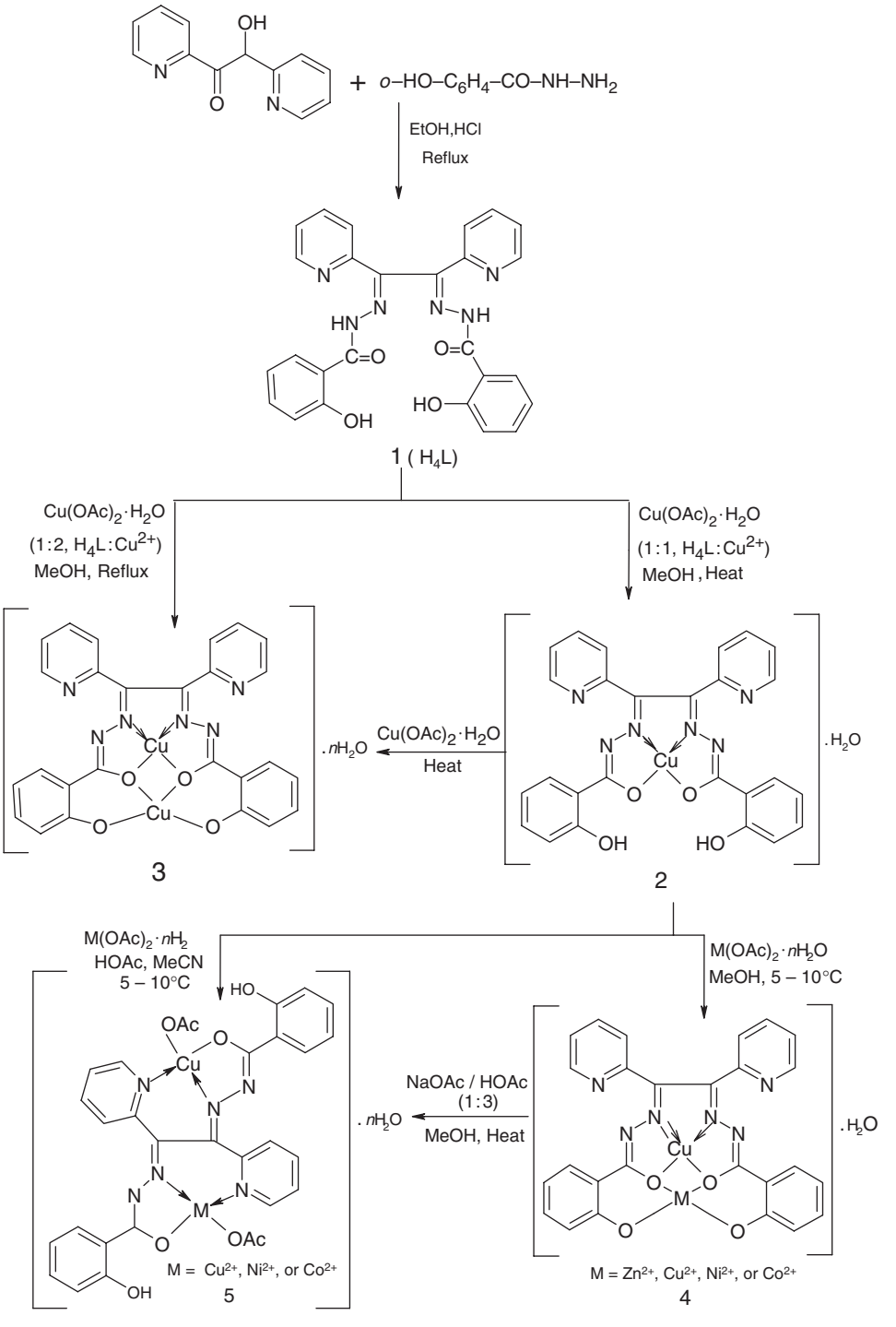

Figure 1. Synthesis of H_4L and its metal complexes.

or $C_2H_4Cl_2$ solution were accomplished on a Varian Cary-5 double beam spectrometer. Magnetic susceptibilities were measured by the Faraday balance as described before [11]. Thermal analyses were carried out on a Shimadzu Thermal system 50 consisting of TGA-50 and DTA-50 from room temperature to 1000°C under nitrogen with a heating rate of $10^{\circ}C\,min^{-1}$. The molar conductivity was measured for 1.00×10^{-3} DMF solutions at $25^{\circ}C \pm 1^{\circ}C$ using a Jenway 4020 conductivity meter.

2.4. *Screening for antibacterial activity*

H_4L and complexes were screened *in vitro* for their antibacterial activity against five Gram-positive (*Staphylococcus aureus*, *Staphylococcus hominis*, *Bacillus sp 1*, *Bacillus sp 2,* and *Bacillus sp 3*) and three Gram-negative (*Escherichia coli*, *Salmonella sp 1*, and *Salmonella sp 2*) bacterial strains using gel diffusion and respirometric methods. The gel diffusion method was used as previously described [12]. Bacterial cultures were grown overnight on nutrient agar (NA) plates. Bacterial biomass was suspended in 0.9% saline and adjusted to an optical density (OD) of 0.02 at $\lambda = 600$ nm. Bacterial suspensions were spread on the NA plates using sterile cotton swabs. Uniform wells were created in the NA plates using a cork-borer (6 mm). Test compounds were transferred (100 µL, 0.1 mg) into the wells and ethanol was used as control. Plates were incubated for 24 h at 37°C and the diameter of inhibition zones around the wells are measured in centimeters. Each test was conducted in triplicate and the mean with standard deviation was calculated. The inhibitory effects of synthesized H_4L and metal(II) complexes on bacterial respiration were also investigated using the previously reported method [13–16]. Compounds (0.5 and 1 mg) were transferred to sterile bottles containing 49 mL nutrient broth and bacterial culture (1 mL of overnight culture, OD 1 at $\lambda = 600$ nm). Bottles were connected to a respirometer (Micro-Oxymax Columbus Instruments) and incubated in a shaking water bath at 37°C. Bottles with sterile nutrient broth were used as control. Experiments were conducted in triplicate and the amount of carbon dioxide evolved was plotted against time. In order to clarify any participating role of DMSO in the biological screening, separate studies were carried out with the solutions without the complexes and they showed less or no activity against bacteria.

2.5. *Computational procedures*

All calculations were carried out on a Pentium IV 3.2 GHz machine on windows XP using HyperChem release 7 [17]. The geometry was energetically optimized through molecular mechanics applying MM^+ force field in vacuum with the polka Ribiere (conjugated gradient) algorithm and RMS gradient $0.001\,kcal\,mol^{-1}$ followed by molecular dynamics. The optimization is performed without constraints allowing all atoms, bonds, and dihedral angles to change simultaneously. The dynamic was done up to 2000 K followed by molecular mechanics calculations and same process was repeated five times to ensure the energy minimum had been reached. A bath of relaxation time of 0.1 ps and a step size of 0.001 ps were used for dynamics simulation.

3. Results and discussion

3.1. *General*

Homo- and heterobinuclear copper(II) complexes $[CuLM]\cdot nH_2O$ and $[Cu(H_2L)M(OAc)_2]\cdot nH_2O$, where $M = Zn^{2+}$, Cu^{+2}, Ni^{2+}, or Co^{2+}; L and H_2L are the anionic forms of dipyridylglyoxal *bis*(2-hydroxybenzoyl hydrazone) and $n = 1$–2, were synthesized according to figure 1. Good yield and pure products were obtained by the reaction of $[(H_2L)Cu]\cdot H_2O$ with the appropriate hydrated metal(II) acetate. Low temperatures and short reaction times are necessary to isolate pure heterobinuclear compounds. At high temperature and/or longer time, the heterobinuclear were dissociated according to the reaction:

$$2[CuLM]\cdot nH_2O \rightarrow [Cu_2L]H_2O + [M_2L\cdot nH_2O]$$

The complexes $[CuLM]\cdot nH_2O$, where $M = Zn^{2+}$, Cu^{+2}, Ni^{2+}, or Co^{2+}, are insoluble in most organic solvents and water but soluble in DMF, DMSO, CH_3CN, and $C_2H_4Cl_2$, while acetato complexes $[Cu(H_2L)M(OAc)_2]\cdot nH_2O$ are soluble in DMF, DMSO, and Py. The molar conductivities of all complexes at $25^\circ C \pm 1^\circ C$ indicate non-electrolytes [11].

3.2. *FT-IR spectra*

FT-IR spectra of the ligand and its complexes as KBr discs are given in table 2. H_4L displays a broad band centered at $3438\,cm^{-1}$ which could be assigned to hydrogen bonded O–H. The presence of a broad weak band at $1917\,cm^{-1}$ could be taken as evidence for the presence of an intramolecular hydrogen bond O–H···O, confirmed by the appearance of a phenolic ν(C–O) at $1279\,cm^{-1}$.

For $[CuLM]\cdot nH_2O$, the OH feature at $3438\,cm^{-1}$ is absent and ν(C–O) shifts $\sim 20\,cm^{-1}$ to higher energy, suggesting bonding of the phenolato-oxygen to the metal [12]. Spectra of $[(H_2L)Cu]\cdot nH_2O$ and $[Cu(H_2L)M(OAc)_2]\cdot nH_2O$ exhibit ν(C–O) at 1283–$1276\,cm^{-1}$ and ν(OH) at 3440–$3431\,cm^{-1}$, suggesting that phenolic OH is not bonded to the metal. The spectrum of H_4L shows strong bands at 1625 and $1583\,cm^{-1}$ characteristic of ν(C=N) of the azomethine and pyridine, respectively. The appearance of a single band for azine and pyridine suggests that the ligand is symmetrical.

The spectrum of the free ligand exhibits a medium sharp band at $3274\,cm^{-1}$ characteristic of ν(NH). Upon complex formation, ν(C=N) of pyridine is at 1588–$1580\,cm^{-1}$ indicating non-bonding, while that of azine is at 1600–$1596\,cm^{-1}$ due to coordination to metal. The bands at 3274 and $1648\,cm^{-1}$ due to ν(NH) and ν(C=O) in the free ligand are absent in all complexes with the appearance of a new medium-strong band at 1628–$1630\,cm^{-1}$, attributed to the formation of the conjugate system C=N–N=C through enolization of the keto group with the adjacent –NH–, suggesting bonding of the enolato-oxygen to the metal. Therefore, the ligand is ionic tetra- or hexadentate as a N_2O_2 or N_2O_4 donor forming neutral complexes. The spectra of all complexes display a broad band centered at 3489–$3478\,cm^{-1}$ due to the water of crystallization. The far IR spectra of all dinuclear complexes display a series of new bands at 502–512, 354–368, 467–489, and 522–$531\,cm^{-1}$ assigned to $\nu(M–N)_{azine}$, $\nu(M–N)_{pyridine}$, $\nu(M–O)_{hydrazone}$, and $\nu(M–O)_{phenolate}$, respectively. The IR spectra of

Table 2. Main IR bands ($\acute{\upsilon}$, cm^{-1}) with their tentative assignments.

Compound	ν(NH)	ν(OH)	ν(C=N) (Py)	ν(C=N) (azine)	ν(C–O)	ν(M–N) (azine)	ν(M–N) (Py)	ν(M–O)	ν(C=N–N=C)	ν(OAc)
H_4L	3274	3438	1583	1625	1279	–	–	–	–	–
$[(H_2L)Cu]\cdot H_2O$	–	3435	1583	1600	1276	512	–	486	1628	
$[CuLCu]\cdot H_2O$	–	3489	1583	1599	1300	502	–	480, 530	1622	
$[CuLCo]\cdot H_2O$	–	3478	1583	1598	1296	504	–	479, 526	1626	
$[CuLNi]\cdot 2H_2O$	–	3486	1583	1600	1295	506	–	467, 530	1620	
$[CuLZn]\cdot H_2O$	–	3485	1583	1600	1298	504	–	489, 531	1630	
$[Cu(H_2L)Cu(OAc)_2]\cdot H_2O$	–	3439	1583	1598	1280	512w	368	488, 526	1630	1610, 1369
$[Cu(H_2L)Co(OAc)_2]\cdot H_2O$	–	3439	1583	1600	1279	510	355	482, 520	1629	1618, 1373
$[Cu(H_2L)Ni(OAc)_2]\cdot 2H_2O$	–	3440	1583	1600	1280	508	354	479, 522	1629	1616, 1358

$[Cu(H_2L)M(OAc)_2]\cdot nH_2O$ display two new bands at 1610–1618 and 1358–1373 cm^{-1} assignable for $\nu(COO)_{asym}$ and $(COO)_{sym}$, respectively. Values of $\Delta\acute{\upsilon} = \nu(COO)_{asym}$ and $(COO)_{sym} = 241–258\,cm^{-1}$ indicate monodentate acetate in these complexes [18]. IR data, elemental analyses, and molar conductivity confirm the structures in figure 1.

3.3. *Magnetic and electronic spectral studies*

The electronic spectrum of H_4L as nujol mull exhibits intense bands at 39,000 and 32,750 cm^{-1} due to Ph–Ph* and π–π* transitions, respectively. Lower intensity bands at 27,050 and 26,480 cm^{-1} are assigned to n–π* (pyridine) and n–π* (azomethine) transitions, respectively, which disappear in all complexes and with appearance of a band at 27,755–27,880 for $[CuLM]\cdot nH_2O$ and 27,540–27,100 cm^{-1} for $[Cu(H_2L)M(OAc)_2]\cdot nH_2O$ and $[(H_2L)Cu]\cdot H_2O$, suggesting the coordination of azomethine-nitrogen to metal. In $[Cu(H_2L)M(OAc)_2]\cdot nH_2O$, the n–π* (pyridine) transition disappeared suggesting the bonding of pyridine to metal. These changes in the UV spectral bands are consistent with the IR data.

The electronic spectra of the complexes either as nujol mulls or $C_2H_4Cl_2$ solution are similar and therefore the solution spectral data are given in table 3. The spectrum of $[(H_2L)Cu]\cdot H_2O$ displays one d–d transition at 18,275 cm^{-1} as reported for square planar copper(II) complexes with N_2O_2 donors [13, 19–21]. The spectrum of $[CuLCu]\cdot H_2O$ has two d–d transitions at 18,470 and 16,540 cm^{-1} characteristic of square planar copper(II) complexes with different sets of donors. The higher energy band is similar to that obtained in $[(H_2L)Cu]\cdot H_2O$ due to CuN_2O_2, therefore the lower energy band is assumed as CuO_4. The presence of CuO_4 is also confirmed by a new intense band at 25,000 cm^{-1} characteristic of O $(p_\pi) \rightarrow$ Cu (d_π) [13, 19–21].

The spectrum of $[CuLNi]\cdot 2H_2O$ shows bands at 21,850 and 19,000 cm^{-1}, consistent with those reported for square planar nickel (II) and copper(II) complexes. The lower energy band is comparable to that obtained for CuN_2O_2 and the higher energy band is due to NiO_4 chromophore. This is supported by the appearance of a new band at 25,285 cm^{-1} assigned to O $(p_\pi) \rightarrow$ Ni (d_π) [13, 19–21].

$[CuLCo]\cdot H_2O$ displays d–d transitions at 14,900, 15,400, and 18,880 cm^{-1} and a more intense new band at 25,300 cm^{-1}. The band at 18,380 cm^{-1} is similar to $[(H_2L)Cu]\cdot nH_2O$, $[CuLCu]\cdot H_2O$, and $[CuLNi]\cdot 2H_2O$ and, therefore, assigned to square planar CuN_2O_2. The two new bands at 14,900 and 15,400 cm^{-1} are due to

Table 3. Room temperature magnetic moment values (μ_{eff}, B.M.) and electronic spectral data.

Compound	μ_{eff}	Electronic transitions, cm^{-1} ($\log\varepsilon$, $L\,mol^{-1}\,cm^{-1}$)
H_4L[a]		39,000, 32,750, 27,050, 26,480
$[(H_2L)Cu]\cdot H_2O$	1.79	27,100 (3.79), 18,275 (2.31)
$[CuLCu]\cdot H_2O$	1.19	27,880 (3.84), 25,000 (3.36), 18,470 (2.33), 16,540 (2.11)
$[CuLCo]\cdot H_2O$	4.12	27,855 (3.77), 18,880(2.03), 15,400 (3.94), 14,900 (3.22)
$[CuLNi]\cdot 2H_2O$	1.85	27,755 (3.69), 21,850 (2.32), 19,000 (2.29)
$[CuLZn]\cdot H_2O$	1.79	27,765 (3.59), 18,510 (2.19)
$[Cu(H_2L)Cu(OAc)_2]\cdot H_2O$[a]	1.78	27,540, 26,080, 24,980, 22,300, 17,900
$[Cu(H_2L)Co(OAc)_2]\cdot H_2O$[a]	4.96	27,490, 25,970, 24,700, 17,950, 17,000, 16,500, 12,200
$[Cu(H_2L)Ni(OAc)_2]\cdot 2H_2O$[a]	1.86	27,500, 25,670, 24,800, 20,900, 17,500, 14,650

[a]Spectra recorded for saturated solutions.

cobalt(II), and judging from the positions and intensities, the configuration around the cobalt(II) is nearly tetrahedral [22]. The spectrum of $[CuLZn]\cdot H_2O$ shows a band at 18,510 cm^{-1} characteristic of CuN_2O_2 and 25,400 cm^{-1} due to LMCT transition. The intensity of the d–d transition bands of CuN_2O_2 is decreased and blue shifted by introduction of a second metal ion. The extent of the blue shift and intensity loss is in the order: $Zn^{2+} < Co^{2+} < Ni^{2+}$ in the reverse order of their ionic radii of 0.78, 0.74, and 0.70 Å, respectively, attributed to CuN_2O_2 becoming more planar in $[CuLM]\cdot nH_2O$ relative to $[(H_2L)Cu]\cdot H_2O$.

Electronic spectra of $[Cu(H_2L)M(OAc)_2]\cdot nH_2O$, $M = Cu^{2+}$, Ni^{2+} or Co^{2+}, and $n = 1$ or 2 (table 3) exhibit a broad band with a maximum at 17,900 cm^{-1} and a shoulder at 22,300 cm^{-1} for $M = Cu^{2+}$ characteristic of distorted square planar copper(II) complexes. In case of $M = Ni^{2+}$, the spectrum displays bands at 17,500, 14,650, and 20,900 cm^{-1}. The higher energy band is characteristic of distorted square planar copper(II) complexes while the other two bands are consistent with distorted square planar nickel(II) complexes [13, 19–22]. The spectrum of $[Cu(H_2L)Co(OAc)_2]$ displays bands at 12,200, 16,500, 17,000, and 17,950 cm^{-1}. The first three bands are characteristic of a tetrahedral cobalt(II) while that at 17,950 cm^{-1} is attributed to a distorted square planar copper(II). The spectra of all complexes exhibit a band at 24,700–24,980 cm^{-1} with a shoulder at 25,670–26,080 cm^{-1}, which could be attributed to MLCT transitions.

Molecular modeling studies using MM^+ calculations are performed to gain a better understanding of geometrical structures of the investigated complexes. The structures for the complexes were predicted through strain energy, calculated through the molecular mechanics (MM^+) coupled with molecular dynamics calculations. Although the molecular mechanics calculations cannot predict the electronic properties, still it has enormous applications in the field of coordination chemistry [22–24]. Details are provided in "Supplementary material".

The room temperature magnetic moments of $[Cu(H_2L)M(OAc)_2]\cdot nH_2O$ of 1.78, 1.86, and 4.96 B.M. for $M = Cu^{2+}$, Ni^{2+}, and Co^{2+}, respectively, suggest either an uncoupled system or one involving weak spin exchange. The values in the case of $M = Ni^{2+}$ or Zn^{2+} are quite reasonable since Ni^{2+} and Zn^{2+} have no unpaired electron and the value for $M = Co^{2+}$ is a normal value for complexes containing copper(II) and tetrahedral cobalt(II). The room temperature magnetic moment of $[CuLCu]\cdot H_2O$ of 1.19 falling to 0.599 B.M. mol^{-1} at 4 K is consistent with antiferromagnetically coupled copper(II) complexes [2, 3]. The temperature dependence of the magnetic susceptibility of this complex in the temperature range 300–4 K showed that the susceptibility passes through a maximum at 30 K and then decreases with increasing the temperature, typical for an antiferromagnetically coupled system. The fit to the experimental data was performed according to the Hamiltonian: $H_{ex} = -2J_{12}(S_{Cu1}S_{Cu2})$, where J_{12} is the exchange coupling parameter between the copper centers. The magnetic susceptibility χ_M is derived from the Hamiltonian, according to Kahn [25].

$$\chi_M = \left[2N_A\beta^2g^2/3K(T-\theta)\right]\left[(1-\rho)/3\exp^{-2J/KT}+\rho/4\right],$$

where T is the absolute temperature, N_A is Avogadro's number, K is Boltzmann's constant, β is the Bohr magneton, θ is a constant which takes into account any additional magnetic effects and is obtained from the extrapolation of χ_M–T plot in the lattice = −32 K, g is the Lande splitting factor, and ρ is the concentration of the

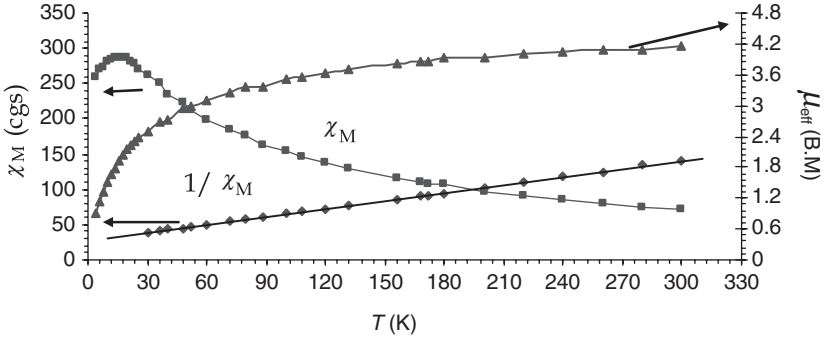

Figure 2. Effect of temperature on the molar magnetic susceptibility (χ_M), $1/\chi_M$, and the effective magnetic moment of $[CuLCo]\cdot H_2O$.

paramagnetic impurities. A best match of the calculated to experimental curve is obtained with magnetic parameters of $g = 2.056$, $J = -318\,cm^{-1}$, and $\rho = 0.011$. The large negative J value indicates strong antiferromagnetic interaction between the copper spins through the bridges, falling into the low limit of the usual range of dimeric copper(II) bridged by μ-phenoxo or μ-hydroxo bridges [26–28]. The smaller absolute value of J relative to that reported for similar dinuclear complexes could be attributed to the distortion of CuO_4 chromophore from planarity as indicated from the electronic spectral data.

The magnetic behavior of $[CuLCo]\cdot H_2O$ in the temperature range 4–300 K is indicative of an overall antiferromagnetic interaction (figure 2). The μ_{eff} at 298 K of 4.124 BM is further evident for such interaction. At 4 K, the magnetic moment is decreased to 0.913 BM compared to 2.87 BM expected for $S_T = 1$. This magnetic interaction is assumed to be between Copper and Cobalt through the bridging group, and the magnetic analysis is carried out using the theoretical expression of susceptibility deduced from the spin Hamiltonian: $H_{ex} = -2J_{12}(S_{Cu}S_{Co})$, where J_{12} is the exchange coupling parameter between the copper and cobalt centers in the dimer. The magnetic susceptibility data is best fitted by using the equation:

$$\chi_M = \left[N_A\beta^2 g^2/K(T-\theta)\right]\left[10 + 2\exp^{(-4J/KT)}/5 + 3\exp^{(-4J/KT)}\right] + N_\alpha,$$

where N_α is the temperature-independent paramagnetism $= 180 \times 10^{-6}$ cm^3 mol^{-1} and $\theta = -29.8$ K. The best fit to the experimental data gives $J = -178\,cm^{-1}$ and $g = 2.48$. The negative values of J and θ suggest that the interaction between the copper and cobalt is antiferromagnetic. The relatively large value of g is consistent with average g values quoted in square planar and tetrahedral ligand fields.

3.4. *Thermal studies*

The DTG results of the ligand and its complexes are given in "Supplementary material". The ligand decomposes in three successive steps with mass loss of 37.81% (at 206°C), 11.28% (at 348°C), and 50.48% (at 489°C) with total estimated mass loss of 99.35% due to the loss of $C_{12}H_{10}N_2$, $2N_2$ and $2C_7H_4O_2$, respectively.

The decompositions of $[(H_2L)Cu]\cdot H_2O$ and $[CuLM]\cdot nH_2O$ are similar: (i) decomposition within the temperature range 96–108°C with estimated loss of 2.61–5.00% attributable to the loss of one or two water molecules, (ii) decomposition within the temperature range 389–402°C with mass loss of 29.00–33.33% due to the loss of $C_{12}H_{10}N_2$, (iii) mass loss of 9.03–9.86% in the 478–572°C range assigned to the loss of two dinitrogens, and (iv) the fourth step at 603–778°C with 37.59–42.66% from the loss of $2C_7H_4O_2$.

The DTG of $[Cu(H_2L)M(OAc)_2]\cdot nH_2O$ exhibit decomposition steps similar to acetato free complexes, but with the addition of an endothermic peak at 388–347°C due to the loss of $2CH_3COO$ and $C_{12}H_{10}N_2$ rather than only $C_{12}H_{10}N_2$.

3.5. *Biological activity*

Antibacterial activity of H_4L, $[(H_2L)Cu]\cdot H_2O$, and $[CuLM]\cdot nH_2O$, $M = Zn^{2+}$, Cu^{2+}, Ni^{2+}, or Co^{2+} and $n = 1$ or 2, are given in Supplemental material. The complexes exhibit inhibitory effects towards Gram-positive and Gram-negative bacteria while the ligand is biologically inactive, but are inactive towards *Salmonella sp 2* and only $[CuLM]\cdot H_2O$, $M = Cu^{2+}$ or Zn^{2+}, and $[(H_2L)Cu]\cdot H_2O$ are active towards *S. aureus*. Antimicrobial inhibitions were compared to the antimicrobial activity of Ofloxacin, showing that $[CuLCu]\cdot H_2O$ and $[(H_2L)Cu]\cdot H_2O$ exhibit comparable activities to Ofloxacin antibiotics. As previously reported, metal salts do not exhibit antimicrobial activity [29–33]. According to the data given in Supplemental material, antimicrobial activity can be ordered as: $[CuLCu]\cdot H_2O > [(H_2L)Cu]\cdot H_2O > [CuLZn]\cdot H_2O > [CuLNi]\cdot 2H_2O \approx [CuLCo]\cdot H_2O$, suggesting that lipophilic behavior increases in the same order. Since all complexes have the same donating atoms with the same coordination number, the same chelate effect (each metal ion forms two five-membered chelating rings), all are neutral and all have the same oxidation number in their complexes, the effective factors are the geometrical shape and the nature of the central atoms. Spectral and magnetic studies indicate that copper has a tetragonal distortion (distorted to a square planar geometry), nickel and cobalt have a square planar and tetrahedral geometry, respectively, while zinc is tetrahedral. Therefore, the antimicrobial activity can be referred to similar structures with the presence of copper. The structures may increase lipophilicity by decreasing the effective nuclear charge (polarity) of $[CuLCu]\cdot H_2O$, $[(H_2L)Cu]\cdot H_2O$, and $[CuLZn]\cdot H_2O$ more than $[CuLNi]\cdot 2H_2O$ and $[CuLCo]\cdot H_2O$. The higher antimicrobial activity of copper(II) complexes relative to zinc(II) complex may be attributed to copper(II) forming a stronger ligand bond than Zn(II), increasing the lipophilic character of copper(II) complexes. Several metal complexes of hydrazone derivatives were screened for their biological and physiological activities against different bacterial and fungal species. Neelamma *et al.* [34] showed that 2-formyl propanal-1H-benimidazole-2-yl-hydrazone and its metal complexes are active against *E. coli* and *S. aureus*. The biological activity studies of diacetyl benzaldehyde acyldihydrazones and succinic acid hydrazones as well as their metal complexes showed significant antifungal activity and fair antibacterial activity especially against *Bacillus* and *Pseudomonas* fluorescence [35, 36]. Singh *et al.* [37] reported that metal complexes of *p*-aminoacetophenone salicyloylhydrazone exhibited a fair degree of antifungal activity against *Aspergillus* sp., *Stemphylium* sp., and T*richoderma* sp. but moderate antibacterial activity against *E. coli* and *Clostridium* sp. Furthermore, the

Table 4. Effect of H_4L and its complexes on the respiration of bacteria.[a]

Compound	Amount (mg)	Bacteria							
		S. aureus	*S. hominis*	*B. sp 1*	*B. sp 2*	*B. sp 3*	*E. coli*	*S. sp 1*	*S. sp 2*
$[(H_2L)Cu]\cdot H_2O$	0.5	77 ± 3	–	95 ± 6	53 ± 3	84 ± 6	68 ± 5	41 ± 2	–
	1.0	92 ± 4	–	93 ± 6	94 ± 3	86 ± 6	89 ± 3	79 ± 5	–
$[CuLCu]\cdot H_2O$	0.5	94 ± 5	88 ± 6	97 ± 6	94 ± 6	88 ± 6	93 ± 6	91 ± 4	–
	1.0	94 ± 6	91 ± 6	95 ± 6	95 ± 4	91 ± 6	94 ± 6	92 ± 5	–
$[CuLNi]\cdot 2H_2O$	0.5	–	–	59 ± 5	79 ± 4	45 ± 2	37 ± 2	–	–
	1.0	–	16 ± 1	89 ± 6	91 ± 6	67 ± 4	59 ± 4	–	–
$[CuLCo]\cdot H_2O$	0.5	–	–	27 ± 2	36 ± 2	33 ± 2	40 ± 5	–	–
	1.0	–	–	70 ± 5	79 ± 5	70 ± 5	60 ± 3	–	–
$[LCuZn]\cdot H_2O$	0.5	66 ± 3	75 ± 5	82 ± 2	59 ± 3	55 ± 1	78 ± 5	55 ± 3	–
	1.0	87 ± 6	89 ± 6	84 ± 3	75 ± 5	88 ± 5	78 ± 5	88 ± 6	–

[a]Results represent percent inhibition of bacterial respiration caused by the addition of 0.5 and 1.0 mg of the test compound. Results are the mean of three independent analyses with standard deviations.

complexes of *p*-aminoacetophenone isonicotinoyl hydrazone [38] showed fair antifungal activity against *Rizoctonia* sp., *Aspergillus* sp., *Stemphylium* sp., and *Penicillium* sp. and appreciable antibacterial activity against *Pseudomonas* sp. and *E. coli*. Antibacterial screening data of the trinuclear Cu(II)/Ni(II) complexes with pentadentate ligand *N*-2-methyl-acryloyl-salicylhydrazide, as well as their corresponding mononuclear copper and tetranuclear nickel complexes against *S. aureus*, *E. coli*, *B. subtilis*, and *P. vulgaris* [39], showed that the two trinuclear complexes have stronger antimicrobial activities against the tested microorganisms than ligand. The trinuclear copper compound is more active than monocopper compounds, and the trinuclear nickel compound is less active than tetranuclear nickel compound.

Data on antibacterial activity of four trinuclear copper(II) and nickel(II) complexes with pentadentate ligands derived from *N*-acylsalicylhydrazide against *S. aureus*, *E. coli*, *B. subtilis*, and *P. vulgaris* indicated that the ligands are inactive to the entire array of tested microorganism while complexes have strong antimicrobial activities (tables 4 and 5) [40].

4. Conclusion

The homo- and heterobinuclear complexes $[CuLM]\cdot nH_2O$, where L is the anion of dipyridylglyoxal *bis*(2-hydroxybenzoyl hydrazone), H_4L, M = Cu(II), Co(II), Ni(II), or Zn(II) and $n = 1$ or 2, were synthesized and characterized. IR data suggest that H_4L is dibasic tetradentate in $[(H_2L)Cu]\cdot H_2O$ and $[Cu(H_2L)M(OAc)_2]\cdot nH_2O$ but tetra-basic hexadentate in $[CuLM]\cdot nH_2O$, $n = 1$–2. CuN_2O_2 in all complexes is a tetragonal distorted structure (mainly square planar), while the second metal ion (MO_4 chromophore) is tetrahedral or distorted square planar. The heterobinuclear complexes with M = Cu(II) or Co(II) exhibit strong antiferromagnetic interactions with $J = -318$ and $-178\,cm^{-1}$, respectively. The heterobinuclear complexes $[Cu(H_2L)M(OAc)_2]\cdot nH_2O$

Table 5. Antimicrobial results (zone of inhibition, diameter in cm) of $[(H_2L)Cu]\cdot H_2O$ and $[CuLM]\cdot nH_2O$ gel diffusion method.

	Bacteria							
Compound	*S. aureus*	*S. hominis*	*B. sp 1*	*B. sp 2*	*B. sp 3*	*E. coli*	*S. sp 1*	*S. sp 2*
$[(H_2L)Cu]\cdot H_2O$	2.48 ± 0.02	–	2.99 ± 0.05	3.00 ± 0.10	1.96 ± 0.11	2.29 ± 0.10	1.76 ± 0.04	–
$[CuLCu]\cdot H_2O$	2.62 ± 0.03	2.48 ± 0.04	3.25 ± 0.10	3.09 ± 0.06	2.21 ± 0.06	2.98 ± 0.04	3.01 ± 0.04	–
$[CuLNi]\cdot 2H_2O$	1.20 ± 0.04	1.00 ± 0.03	0.90 ± 0.03	0.90 ± 0.03	1.00 ± 0.04	–	1.40 ± 0.05	–
$[CuLCo]\cdot H_2O$	0.90 ± 0.03	1.00 ± 0.03	1.20 ± 0.04	1.20 ± 0.04	0.90 ± 0.03	0.90 ± 0.03	–	–
$[LCuZn]\cdot H_2O$	1.98 ± 0.01	2.02 ± 0.01	2.65 ± 0.02	2.68 ± 0.03	1.91 ± 0.02	2.48 ± 0.01	2.47 ± 0.10	–
Ofloxacin	1.90 ± 0.11	2.81 ± 0.04	0.28 ± 0.01	0.28 ± 0.03	–	1.20 ± 0.13	0.15 ± 0.01	0.16 ± 0.02

consist of two CuN_2O_2 and MN_2O_2 chromophores with a very weak or negligible magnetic interaction. The antimicrobial activities of $[CuLM]\cdot nH_2O$ against some Gram-positive and Gram-negative bacterial species, the antimicrobial activities can be ordered as: $[CuLCu]\cdot H_2O > [(H_2L)Cu]\cdot H_2O > [CuLZn]\cdot H_2O > [CuLNi]\cdot 2H_2O \approx [CuLCo]\cdot H_2O$.

Acknowledgement

The authors would like to acknowledge Kuwait University for the general facility projects grant Nos GS01/01 and GS03/01.

References

[1] R. Kruszynski, B. Machura, M. Wolff, J. Kusz, J. Mroziński, A. Bieńko. *Inorg. Chim. Acta*, **362**, 1369 (2009).
[2] A. El-Dissouky, G.B. Muhammad. *Inorg. Chim. Acta*, **168**, 241 (1990).
[3] A. El-Dissouky, A.Z. El-Sonbati. *Polyhedron*, **9**, 2443 (1990).
[4] W.R. Browne, R. Hage, J.G. Vos. *Coord. Chem. Rev.*, **250**, 1653 (2006).
[5] V. Rajendiran, R. Karthik, M. Palaniandavar, H. Stoeckli-Evans, V. Subbarayan Periasamy, M.A. Akbarsha, B.S. Srinag, H. Krishnamurthy. *Inorg. Chem.*, **46**, 8208 (2007).
[6] M. Trivedi, D.S. Pandey, N.P. Rath. *Inorg. Chim. Acta*, **362**, 284 (2009).
[7] T. Rüffer, B. Bräuer, F.E. Meva, L. Sorace. *Inorg. Chim. Acta*, **362**, 563 (2009).
[8] A.M. Madalan, V. Ch. Kravtsov, D. Pajic, K. Zadro, Y.A. Simonov, N. Stanica, L. Ouahab, J. Lipkowski, M. Andruh. *Inorg. Chim. Acta*, **357**, 4151 (2004).
[9] E.Q. Gao, J.K. Tang, D.Z. Liao, Z.H. Jiang, S.P. Yan, G.L. Wang. *Inorg. Chem.*, **40**, 3134 (2001).
[10] M.K. Awad, A.K. Shehata, A. El-Dissouky. *Transition Met. Chem.*, **20**, 448 (1995).
[11] W.J. Geary. *Coord. Chem. Rev.*, **7**, 81 (1971).
[12] J. Welby, L.N. Rusere, J.M. Tanski, L.A. Tyler. *Inorg. Chim. Acta*, **362**, 1405 (2009).
[13] P.A. Vigato, V. Peruzzo, S. Tamburini. *Coord. Chem. Rev.*, **253**, 1099 (2009).
[14] P.C. Fuchs, R.N. Jones, A.L. Barry. *J. Clin. Microbiol.*, **28**, 608 (1990).
[15] K.J. Ryan, G.M. Needham, C.L. Dunsmoor, J.C. Sherris. *Appl. Microbiol.*, **20**, 447 (1970).
[16] A. Adiguzel, H. Ozer, H. Kilic, B. Cetin. *Czech. J. Food Sci.*, **25**, 81 (2007).
[17] HyperChem, release 7 for Windows, Molecular Modeling System, Copyright 2002, Hypercube, Inc.
[18] K. Nakamoto. *Infrared and Raman Spectra of Inorganic and Coordination Compounds, Part B*, 5th Edn, p. 59, John Wiley & Sons Inc., New York, USA (1997).
[19] M. Basato, M. Bortolussi, E. Faggin, C. Tubaro, A.C. Veronese. *Inorg. Chim. Acta*, **362**, 531 (2009).
[20] S. Tanase, M. Viciano-Chumillas, J.M.M. Smits, R. de Gelder, J. Reedijk. *Polyhedron*, **28**, 457 (2009).
[21] E.I. Solomon, A.B.P. Lever. *Inorganic Electronic Structure and Spectroscopy: Applications and Case Studies*, Vol. 2, John Wiley & Sons, New York, USA (2006).
[22] B.P. Hay, R.D. Hancock. *Coord. Chem. Rev.*, **212**, 61 (2001).
[23] M. Zimmer. *Chem. Rev.*, **95**, 2629 (1995).
[24] S. de Silva, R. de Silva, K. Silva. *J. Mol. Struct. (Theochem.)*, **711**, 73 (2004).
[25] O. Kahn. *Molecular Magnetism*, VCH, Weinheim (1993).
[26] C.J. Calzado, J. Cabrero, J.P. Malrieu, R. Caballol. *J. Chem. Phys.*, **16**, 2728 (2002).
[27] M.F. Haddow, H. Kara, G.R. Owen. *Inorg. Chim. Acta*, **362**, 3502 (2009).
[28] Md. Mijanuddin, A.D. Jana, M.G.B. Drew, C.S. Hong, B. Chattopadhyay, M. Mukherjee, M. Nandi, A. Bhaumik, M. Helliwell, G. Mostafa, M. Ali. *Polyhedron*, **28**, 665 (2009).
[29] B. Jeragh, A. El-Dissouky. *J. Coord. Chem.*, **12**, 1029 (2005).
[30] E.K. Efthimiadou, G. Psomas, Y. Sanakis, N. Katsaros, A. Karaliota. *Inorg. Biochem.*, **101**, 525 (2007).
[31] K.Z. Ismail, A. El-Dissouky, A.K. Shehata. *Polyhedron*, **16**, 2909 (1997).
[32] A.D. Russell. In *Densification, Sterilization and Preservation*, S.S. Block (Ed.), 4th Edn. pp. 27–59 and 290–231, Lee and Febinger, Philadelphia, PA (1991).
[33] Z.H. Chohan. *Appl. Organomet. Chem.*, **20**, 112 (2006).
[34] M. Neelamma, P.V. Rao, V. Jyothi. *Int. J. Pure Appl. Chem.*, **2**, 205 (2007).

[35] P.V. Singh, P. Gupta. *J. Coord. Chem.*, **61**, 3922 (2008).
[36] P.V. Singh, P. Gupta. *Pharm. Chem. J.*, **42**, 196 (2008).
[37] P.V. Singh, A. Katiyar. *J. Coord. Chem.*, **61**, 3200 (2008).
[38] P.V. Singh, A. Katiyar, S. Singh. *J. Coord. Chem.*, **62**, 1336 (2009).
[39] W. Luo, X.-G. Meng, G.-Z. Cheng, Z.-P. Ji. *Inorg. Chim. Acta*, **362**, 551 (2009).
[40] W. Luo, X.-G. Meng, J.-F. Xiang, Y. Duan, G.-Z. Cheng, Z.-P. Ji. *Inorg. Chim. Acta*, **361**, 2667 (2008).